Dynamics of coherent optical pumping in a sodium atomic beam

E. A. Korsunsky, W. Maichen, and L. Windholz
Institut für Experimentalphysik, Technische Universität Graz, A-8010 Graz, Austria
(Received 26 December 1996)

This work is concerned with the temporal evolution of the coherent population trapping (CPT) process in the case of additional optical pumping to states not contributing to the CPT superposition states. Special attention is paid to the influence of weak external magnetic fields that can change the laser-atom interaction considerably. The theoretical analysis is completed by experimental observations on a sodium atomic beam, which show good agreement with our theory. The results obtained are of importance for a realistic picture of CPT schemes in practical applications. [S1050-2947(97)08110-9]

PACS number(s): 32.80.Pj, 42.50.Vk

I. INTRODUCTION

Coherent optical pumping (COP) [1] is referred to as a process in realistic laser-atom interaction schemes where optical pumping and coherent population trapping [2] are combined. The simplest model for coherent population trapping (CPT) includes a three-level Λ atomic system, where a specific coherent superposition of two ground states is formed. This superposition is completely decoupled from the laser field at two-photon resonance. The population of the system is optically pumped into this noncoupled (which is also called ''dark'') state and trapped there. A large number of different applications of CPT such as lasing without inversion, electromagnetically induced transparency, and subrecoil cooling of atoms is based on the resonant character of such a trapping. However, it turns out that it is very difficult to find pure Λ systems in real atomic systems. For example, laser excitation of alkali-metal atoms involves tens of Zeeman sublevels. Apart from the Λ-type systems that allow preparation of CPT, there are always some transitions present that do not. Moreover, there could be some ground-state sublevels that are not excited at all. In such a situation, a fraction of atomic population is trapped in specific coherent superpositions and the rest is pumped into other atomic states (COP). This process is more complicated than the CPT establishment in a Λ system, but it is currently of great interest due to applications of the phenomenon in real atoms. In atomic beam experiments [3–5], atoms interact with laser light for a certain time, which is often not sufficiently long for atoms to reach a steady state. Moreover, the state of the atoms changes along the interaction zone. Thus the temporal evolution of atomic populations is very important when examining CPT and COP phenomena. This problem has been considered theoretically by several authors [6–12], but, to the best of our knowledge, was never investigated in experiment. In the present paper we investigate both theoretically and experimentally the dynamics of CPT and COP in a sodium atomic beam excited on the D_1 line by a bichromatic laser beam. Both frequency components have parallel linear polarizations and their frequency difference matches the hyperfine splitting of the $3\,^2S_{1/2}$ ground state of Na so that they are tuned on the $F=1\leftrightarrow F'=2$ and $F=2\leftrightarrow F'=2$ transitions, respectively. In this configuration, two three-level Λ schemes $F=1\leftrightarrow F'=2\leftrightarrow F=2 (m_F=+1$ and $m_F=-1)$ and three two-level schemes $F=1\leftrightarrow F'=2 (m_F=0)$, $F=2\leftrightarrow F'=2 (m_F=+2$ and $m_F=-2)$ are formed and the Zeeman sublevel $F=2$, $m_F=0$ is not excited by the laser radiation (see Fig. 1). The m_F quantum number denotes here the projection of the atomic angular momentum F on the axis parallel to the laser polarization (z axis). The Λ systems are responsible for the creation of CPT and the state $F=2$, $m_F=0$ serves as a sink in the regular optical pumping process. The situation in such a laser-atom interaction scheme depends critically on the presence of a magnetic field [13,14]. The components of the external magnetic field perpendicular to the z axis would induce transitions between Zeeman sublevels of one hyperfine state. In this case all schemes described above get coupled to each other not only by spontaneous emission but also by the magnetic field. Therefore, one should include all sublevels in the analysis. But then the clear physical picture of the process would be lost.

In order to give such a picture and to investigate the main features of coherent optical pumping we start with the analysis of the temporal evolution in a single closed Λ system [Fig. 2(a)]. This gives us basic ideas about the establishment process of CPT. We proceed then with the simplest possible model for COP based on a four-level system consisting of a Λ system with an upper state decaying not only to the states $|1\rangle$ and $|2\rangle$, but also out of the system to the state $|0\rangle$ [Fig.

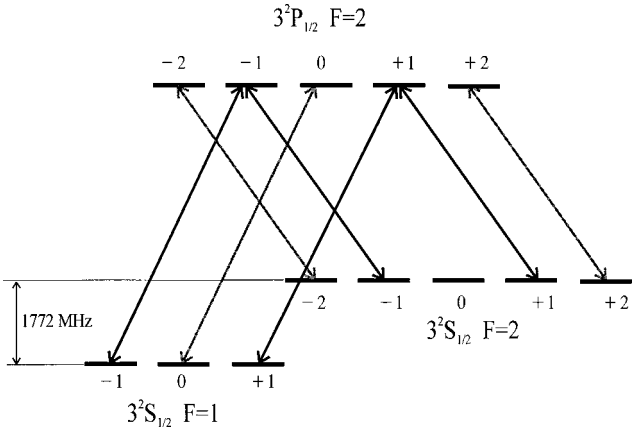

FIG. 1. Relevant structure of the $3\,^2S_{1/2}$ and $3\,^2P_{1/2}$ levels of sodium.

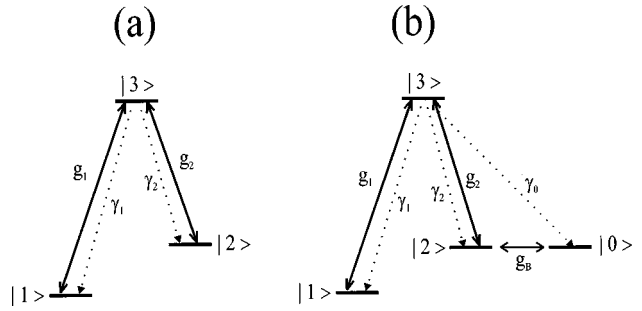

FIG. 2. (a) Three-level Λ system. (b) Four-level system: Λ system with additional radiative decay to external state $|0\rangle$.

2(b)] [1]. This model allows us to outline the most important characteristics of COP. In particular, we investigate the influence of the magnetic field on the temporal evolution of the atomic population under COP conditions. This theoretical analysis is presented in Sec. II. In Sec. III experimental results for time-resolved fluorescence from sodium atoms are given. The measurements are performed both with and without shielding of stray magnetic fields. These results show that the simple four-level model describes qualitatively well the dynamics of COP in a sodium atomic beam. However, good quantitative agreement with the experiment can be obtained only on the basis of calculations involving the complete sodium level scheme of Fig. 1.

II. THEORY FOR Λ AND FOUR-LEVEL SYSTEMS

A. Λ system

Let us consider first the Λ system [Fig. 2(a)] excited by a bichromatic laser field

$$\mathbf{E}=E_1\hat{\mathbf{e}}_z\cos(\omega_1 t)+E_2\hat{\mathbf{e}}_z\cos(\omega_2 t), \tag{1}$$

where $\hat{e}_z$ is the polarization unit vector. We assume that the wave with amplitude E_1 and frequency ω_1 excites only the $|1\rangle$-$|3\rangle$ transition and that with E_2 and ω_2 excites only the $|2\rangle$-$|3\rangle$ transition. The upper state decays spontaneously towards the two ground states $|1\rangle$ and $|2\rangle$ with the rates γ_1 and γ_2, respectively ($\gamma_1+\gamma_2=2\gamma$). In our analysis we also include the decay of coherence between the ground states with the rate Γ. The dynamics of the atomic system is described by the master equation for the density matrix ρ. The process of coherent population trapping is convenient to describe in the basis of coupled $|C\rangle$ and noncoupled $|N\rangle$ states, defined as

$$|C\rangle=\frac{g_1}{g_0}|1\rangle+\frac{g_2}{g_0}|2\rangle, \tag{2}$$

$$|N\rangle=\frac{g_2}{g_0}|1\rangle-\frac{g_1}{g_0}|2\rangle, \tag{3}$$

where $g_m=E_m d_{3m}/2\hbar$ are the Rabi frequencies, d_{3m} are the dipole moments of the $|m\rangle$-$|3\rangle$ transitions ($m=1,2$), and $g_0=\sqrt{g_1^2+g_2^2}$. It follows immediately from the set of the density-matrix equations in this basis (see Ref. [2], for example) that the state $|N\rangle$ is not coupled to the excited state $|3\rangle$ and to state $|C\rangle$ for $\Gamma=0$ and under the two-photon resonance condition

$$\Delta_1=\Delta_2\equiv\Delta. \tag{4}$$

Thus the state $|N\rangle$ becomes a ''perfect trap'' for the atomic population.

One can obtain an exact analytical solution of the three-level problem for the special case of exact resonance $\Delta_1=\Delta_2=0$ and for equal Rabi frequencies $g_1=g_2\equiv g$. Additionally we used the condition

$$\Gamma\ll\gamma, \tag{5}$$

necessary for CPT to be established in a Λ system (i.e., $\rho_{NN}\approx 1$, $\rho_{33}\ll 1$) [2,6]. It is convenient to present the solution for three different ranges of laser intensity (the laser intensity is proportional to the squared Rabi frequency $I\sim g_0^2$):

(i) $g^2\gg\gamma^2$,

$$\rho_{NN}(t)=1-\frac{\Gamma}{4\gamma}(1-e^{-\gamma t/2})-(1-\rho_{NN}^0)\times\left(e^{-\gamma t/2}+\frac{\gamma}{4\sqrt{2}g}\sin(2\sqrt{2}gt)e^{-5\gamma t/4}\right), \tag{6a}$$

$$\rho_{33}(t)=\frac{\Gamma}{4\gamma}(1-e^{-\gamma t/2})+\frac{1}{2}(1-\rho_{NN}^0)\left[e^{-\gamma t/2}-\left(\cos(2\sqrt{2}gt)+\frac{3\gamma}{8\sqrt{2}g}\sin(2\sqrt{2}gt)\right)e^{-5\gamma t/4}\right]; \tag{6b}$$

(ii) $\gamma^2\gg g^2\gg\gamma\Gamma$,

$$\rho_{NN}(t)=1-(1-\rho_{NN}^0)\left(e^{-2g^2t/\gamma}-\frac{2g^2}{\gamma^2}\times(e^{-2g^2t/\gamma}+e^{-2\gamma t}-2e^{-\gamma t})\right), \tag{7a}$$

$$\rho_{33}(t)=\frac{\Gamma}{4\gamma}(1-e^{-2g^2t/\gamma})+(1-\rho_{NN}^0)\frac{2g^2}{\gamma^2}\times(e^{-2g^2t/\gamma}+e^{-2\gamma t}-2e^{-\gamma t}); \tag{7b}$$

and (iii) $g^2\ll\gamma\Gamma$,

$$\rho_{NN}(t)=\frac{1}{2}-\left(\frac{1}{2}-\rho_{NN}^0\right)e^{-2\Gamma t}-\frac{g^2}{\gamma^2}(1-2\rho_{NN}^0)\times(2e^{-2\Gamma t}+e^{-2\gamma t}-3e^{-\gamma t}), \tag{8a}$$

$$\rho_{33}(t)=\frac{g^2}{\gamma^2}\left\{1+2\left[\left(\frac{1}{2}-\rho_{NN}^0\right)e^{-2\Gamma t}+(1-\rho_{NN}^0)\times(e^{-2\gamma t}-2e^{-\gamma t})\right]\right\}. \tag{8b}$$

We have denoted the initial population of the dark state by ρ_{NN}^0 in Eqs. (6)–(8). One can see that CPT is established in a Λ system under the following condition for the laser intensity:

$$g_0^2 \gg \frac{\Gamma}{\gamma}(\gamma^2+\Delta^2). \tag{9}$$

However, the behavior of the atomic populations is different for $g^2 \gg \gamma^2$ and $g^2 \ll \gamma^2$: There are Rabi oscillations with decaying amplitude (the rate of establishment is $\gamma/2$) in the former case and an aperiodical approach of the steady state with the rate $2g^2/\gamma$ in the latter case. Such a behavior closely resembles a regular optical pumping process. The main difference lies in the resonant character of the CPT pumping. Note that if initially atoms are prepared in the dark state $\rho_{NN}^0=1$, the populations nearly do not change, except for small currents of the atomic population proportional to the parameter Γ/γ, which is a measure of imperfection of the CPT. This parameter plays an important role in the CPT phenomenon [2,15,16]. It is obvious from Eqs. (8) that CPT is not reached if the condition (9) is not satisfied, so that CPT cannot be realized at arbitrarily low light intensities. The rate Γ is basically determined by laser fluctuations and atomic collisions. In our atomic beam experiment, the probability of collisions is very low and both laser frequencies are derived from one laser so that they are phase and amplitude correlated. Therefore, the magnitude of Γ is very small in our experiment. However, there are other sources of losses from $|N\rangle$, mainly due to stray magnetic fields and imperfect laser polarizations. We discuss these losses in Sec. II B.

Detuning from the two-photon resonance couples the states $|N\rangle$ and $|C\rangle$. Therefore, the state $|N\rangle$ is not dark anymore and the Λ atoms absorb light. This leads us to the concept of a ''black line,'' which is the region of the two-photon (or Raman) detuning $\delta=\Delta_1-\Delta_2$ where CPT is established. It is the narrow black line that is the basis for numerous applications of the CPT. Therefore, it is interesting to look at the temporal behavior of the black line, i.e., at the dependence of the excited state on both time and two-photon detuning. Figure 3 shows the formation of the black line for the closed Λ system. The contrast of the black line increases with interaction time and approaches 100% (for $\Gamma=0$). We note that in atomic beam experiments one usually measures the fluorescence collected from the whole interaction zone, i.e., the time-averaged signal. Therefore, the contrast and the width of the black line are different from the steady-state values. This difference is commonly neglected in analysis. Such an approach is valid for closed Λ systems and sufficiently long interaction times. In the case of open atomic systems the excited-state population at the steady state is equal to zero for any detuning: The population decays to external states. In this case the transient regime produces the most important contribution to the integrated emitted intensity [17].

B. Four-level system

In our experiment, sodium atoms are excited on the D_1 line by bichromatic linear polarized light. As we discussed in the Introduction, there are two Λ and three two-level systems

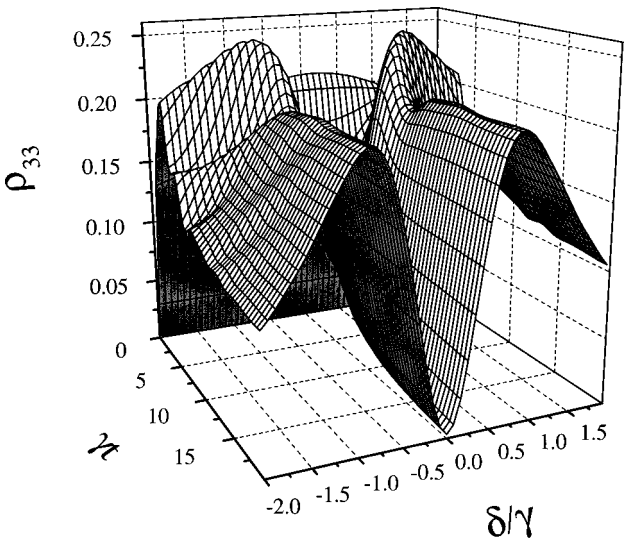

FIG. 3. Temporal evolution of the ''black line'' for the three-level Λ system. Rabi frequencies $g_1=g_2=0.5\gamma$ and the ground-state coherence decay rate $\Gamma=0$.

in this configuration and the Zeeman sublevel $F=2$, $m_F=0$ is not excited (Fig. 1). This is a typical situation of coherent optical pumping: Population is trapped not only in the ''coherent dark'' states of the Λ systems, but also in the ''regular dark'' state $F=2$, $m_F=0$. The simplest atomic system in which COP can be demonstrated is a four-level system [see Fig. 2(b)]: two ground states $|1\rangle$ and $|2\rangle$ that are coupled to the upper state $|3\rangle$ together with an external ground state $|0\rangle$. This system corresponds to one of the Λ systems in Na with the states $|F=1, m_F=1\rangle \doteq |1\rangle$, $|F=2, m_F=1\rangle \doteq |2\rangle$, $|F'=2, m_F=1\rangle \doteq |3\rangle$, and $|F=2, m_F=0\rangle \doteq |0\rangle$ (''$\doteq$'' denotes ''corresponds to''). Atoms decay from the state $|3\rangle$ with rates γ_1, γ_2, and γ_0 to the states $|1\rangle$, $|2\rangle$, and $|0\rangle$, respectively. As we mentioned above, the main contribution to the imperfection of CPT in our experiment are stray magnetic fields. The presence of external magnetic fields considerably complicates the situation since the Zeeman sublevels within each hyperfine state get coupled to each other by transverse components of the field. In order to give a most clear physical picture, we model this coupling in the frame of our four-level system by a precession of the population between states $|2\rangle$ and $|0\rangle$ (between $|F=2, m_F=1\rangle$ and $|F=2, m_F=0\rangle$) with a Larmor frequency $g_B=g_F\mu_B B/\hbar$ ($g_F=\frac{1}{2}$ is the Landé factor of the ground state [18]). With this notation we get $g_B=0.07\gamma_e$ for $B=1$ G($\gamma_e=\gamma_1+\gamma_2+\gamma_0=6.3\times10^7$ s^{-1} for Na).

The set of equations for the density-matrix elements of the four-level system under consideration can be found, for example, in Ref. [1]. This set of equations can be solved analytically only for the case of $g_1=g_2\equiv g$, $\Delta_1=\Delta_2=0$, $\Gamma=0$, and $B=0$. The solution is [where the state $|N\rangle$ is determined as in Eq. (3)], for $g^2 \gg \gamma_e^2$,

$$\rho_{NN}(t)=\rho_{NN}^0+(1-\rho_{NN}^0)\left(\frac{\gamma}{\gamma+\gamma_0}(1-e^{-(\gamma+\gamma_0)t/2})\right.$$

$$\left.-\frac{\gamma}{4\sqrt{2}g}\sin(2\sqrt{2}gt)e^{-(5\gamma+2\gamma_0)t/4}\right), \tag{10a}$$

$$\rho_{33}(t)=\frac{1}{2}(1-\rho_{NN}^0)\Big[e^{-(\gamma+\gamma_0)t/2}-e^{-(5\gamma+2\gamma_0)t/4}\times\Big(\cos(2\sqrt{2}gt)+\frac{3\gamma}{8\sqrt{2}g}\sin(2\sqrt{2}gt)\Big)\Big], \quad (10b)$$

and for $g^2 \ll \gamma_e^2$,

$$\rho_{NN}(t)=\rho_{NN}^0+(1-\rho_{NN}^0)\frac{\gamma}{\gamma+\gamma_0}(1-e^{-[8g^2(\gamma+\gamma_0)/(2\gamma+\gamma_0)^2]t})-(1-\rho_{NN}^0)\Big(\frac{4g^2\gamma}{(2\gamma+\gamma_0)^3}(e^{-(2\gamma+\gamma_0)t}-e^{-(2\gamma+\gamma_0)t/2})\Big), \quad (11a)$$

$$\rho_{33}(t)=(1-\rho_{NN}^0)\frac{8g^2}{(2\gamma+\gamma_0)^2}(e^{-[8g^2(\gamma+\gamma_0)/(2\gamma+\gamma_0)^2]t}+e^{-(2\gamma+\gamma_0)t}-2e^{-(2\gamma+\gamma_0)t/2}). \quad (11b)$$

Here, as in the case of the closed Λ system, $\gamma=(\gamma_1+\gamma_2)/2$. This solution exhibits the same temporal behavior of the atomic populations as in the case of the Λ system [cf. Eqs. (6) and (7)], except for the fact that now a part of the population is pumped into the $|0\rangle$ state and the rate of establishment of the steady state is slightly changed. The solution is applicable to the real situation as long as the external magnetic field is negligibly small. The magnetic field coupling of the dark state $|N\rangle$ to the state $|0\rangle$ is determined by the Larmor frequency g_B. Therefore, the pumping rate into $|N\rangle$ should exceed this coupling for CPT to exist in the four-level system

$$g_0^2/\gamma_e \gg g_B \quad (12)$$

[g_0^2/γ_e is approximately the dark state pumping rate for $g_0^2 \ll \gamma_e^2$; cf. Eq. (11)]. Solid curves in Fig. 4 show the temporal evolution of the excited-state population for very small magnetic field $B=14$ mG ($g_B=0.001\gamma_e$) and other parameters corresponding to our actual experimental conditions. The steady-state population of $|3\rangle$ is equal to zero for the case of two-photon resonance $\delta=\Delta_1-\Delta_2=0$, but also when the Raman detuning δ is different from zero (for example, $\delta=\gamma_e$ as in Fig. 4). However, the rates of establishment are different for the two cases since atomic population only decays towards the $|0\rangle$ state in the latter case and towards both dark states $|N\rangle$ and $|0\rangle$ in the former one. This can also be seen from the temporal evolution of the black lines in populations ρ_{33} [Fig. 5(a)] and ρ_{NN}, ρ_{00} [Fig. 5(b)]. At the early stage of the evolution the populations ρ_{NN} and ρ_{00} are almost constant for any two-photon detuning. In course of time, the black line of COP is formed: The atomic population is equally distributed between the states $|N\rangle$ and $|0\rangle$ at two-photon resonance, while it is completely pumped into the state $|0\rangle$ when the Raman detuning δ is different from zero [see Fig. 5(b)]. In contrast to the closed Λ system (see Fig. 3), the fluorescence intensity (which is proportional to ρ_{33}) disappears as the steady state is approached and the recorded signal is only due to the transient regime. The dotted line on

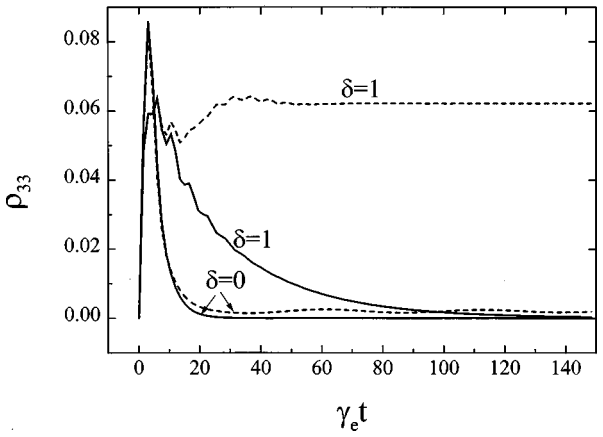

FIG. 4. Excited-state population for the four-level system [Fig. 2(b)] versus time. The parameters correspond to the four-level system $|F=1, m_F=1\rangle$, $|F=2, m_F=1\rangle$, $|F'=2, m_F=1\rangle$, and $|F=2, m_F=0\rangle$, in Na and the total laser intensity $I=26$ mW/cm^2: $\gamma_1=0.41\gamma_e$, $\gamma_2=0.22\gamma_e$, $\gamma_0=0.37\gamma_e$, $g_1=0.36\gamma_e$, and $g_2=0.20\gamma_e$; two-photon detunings δ (in units of γ_e) are denoted at curves. Larmor frequency $g_B=0.001\gamma_e$ ($B=14$ mG), solid curves; $g_B=0.07\gamma_e$ ($B=1$ G), dashed curves.

Fig. 5(a) shows the time-averaged population ρ_{33}, which is usually measured in the experiments.

The dashed curves on Fig. 4 describe the situation for a magnetic field of $B=1$ G ($g_B=0.07\gamma_e$). One can see that CPT is still present at two-photon resonance $\delta=0$ since the condition Eq. (12) is satisfied. The rate of the pumping as well as the steady-state population ρ_{33} are only slightly different from the case of small magnetic fields. But the state $|0\rangle$ is not really dark anymore: The upper state $|3\rangle$ is quickly populated and its population stays constant for $\delta \neq 0$, as it happens, for example, in two-level systems.

III. EXPERIMENT

A. Setup

The temporal behavior of the COP process can be readily studied on an atomic beam where the temporal evolution is translated into a spatial profile. The experimental setup is shown in Fig. 6. The linearly polarized laser beam passes an electro-optical modulator (EOM), which creates sidebands whose frequency difference matches the splitting of the two hyperfine ground levels (1772 MHz for sodium). The sidebands are tuned to the transitions $3\,^2S_{1/2}$, $F=1$ to $3\,^2P_{1/2}$, $F'=2$ and $3\,^2S_{1/2}$, $F=2$ to $3\,^2P_{1/2}$, $F'=2$ of the Na D_1 line, respectively (Fig. 1). By detuning the EOM from the exact match of the splitting one can fulfill or violate the two-photon resonance condition necessary for the establishment of CPT. Therefore, it is possible to compare situations with CPT present and absent, respectively. The laser beam then passes a rectangular slit (S_1), which cuts out an area with nearly homogeneous intensity distribution. Finally, it crosses the atomic beam perpendicularly. The atomic beam is chopped to allow detection via a lock-in technique. For general measurements the light from the whole fluorescence zone is collected by a lens and detected by a photomultiplier tube. In that way one measures the total (integrated) fluorescence during the whole laser-atom interaction. For time-

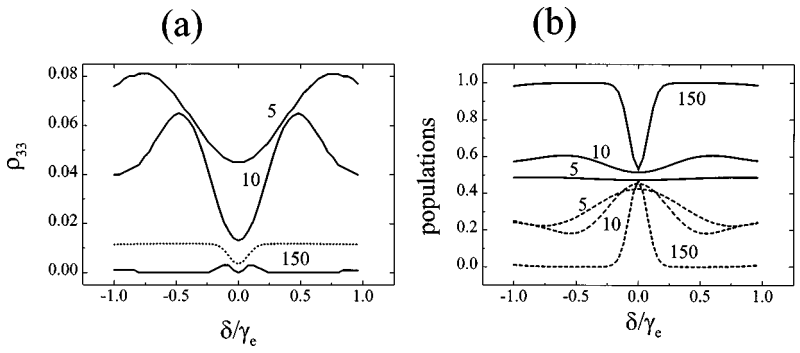

FIG. 5. Black lines for the four-level system at different instants of interaction time (in units of $\gamma_e t$) for $g_B = 0.001\gamma_e$ ($B = 14$ mG). Other parameters are the same as in Fig. 4. (a) Excited-state population; dotted curve, population averaged over the interaction time $t = 150\gamma_e^{-1}$. (b) Populations of the $|N\rangle$ state (dashed lines) and $|0\rangle$ state (solid lines).

resolved measurements the setup is modified: The fluorescence zone is projected onto a rectangular detector slit (S_2, slit width 200 μm) by a lens. The light that falls through this slit is guided to a photomultiplier by an optical fiber. The detector slit, together with the front end of the fiber, is mounted on a stepper motor driven table that can be moved with an accuracy (step width) of 1 μm in the direction of the atomic beam. The signal of the multiplier is recorded by a lock-in amplifier. Data acquisition, as well as the driving of the stepper motor, is performed automatically by a computer.

The picture of the fluorescence zone is enlarged to obtain better spatial resolution despite the finite width of the detection slit. The actual enlargement can be determined by taking the ratio between the laser beam diameter (equal to the width of S_2) and the height of the picture of the fluorescence zone. The atoms have a so-called modified Maxwellian distribution with a mean velocity of 1000 m/s (calculated from the oven temperature of 310 °C). This means that 1 μm along the atomic beam corresponds to 1 ns on the time scale (for mean velocity). As the image of the fluorescence zone is too weak to be visible, the fine adjustment of the lens position is made by maximizing the steepness of the slopes of the scans. Due to residual imperfections of the imaging, the finite detector slit width, and diffraction of the laser beam by the slit S_1, the spatial resolution in the detector plane is limited to approximately 200 μm, corresponding to 200 ns on the time scale.

B. Experimental results

The first series of measurements was taken without any shielding of Earth and stray magnetic field. Therefore, a magnetic field of about 1 G with arbitrary direction was present in the interaction zone. Due to this field the state $F = 2$, $m_F = 0$ is coupled to $F = 2$, $m_F = \pm 1$ and there is no dark state into which atoms could be pumped, as long as CPT is not present. Therefore, the upper levels are always excited and the fluorescence intensity is constant along the whole interaction region. On the other hand, if CPT is present (the two-photon resonance condition is fulfilled), the atoms are pumped into the noncoupled superposition states $|N\rangle_{\pm}$ of the two Λ systems $F = 1 \leftrightarrow F' = 2 \leftrightarrow F = 2 (m_F = \pm 1)$ and the fluorescence decreases along the atomic beam. However, due to the additional magnetic coupling these superpositions are only approximately but not completely decoupled from the exciting laser light and the fluorescence intensity never reaches zero but a finite value. Figure 7 shows two scans of the fluorescence zone: one scan with CPT present (frequency splitting between the two laser light sidebands 1772 MHz) and another without CPT (frequency splitting 1760 MHz, which is outside the region of CPT establishment). The total laser intensity in both sidebands was 120 mW/cm^2. It can be clearly seen that the results match the prediction: Without CPT the intensity stays constant (the slight variation along the beam reflects the varying light intensity across the laser beam), while it decreases with CPT. We note that this behavior is qualitatively well described by our four-level model (cf. dashed curves in Fig. 4). The influence of the optical pumping rate on the time constant for the trapping process was investigated by series of measurements with different laser intensities (Fig. 8). The trapping times T shown in Fig. 8 are obtained from the fluorescence scans by fitting the decay part of the curves by simple exponential decay $I(t) = a \exp[-(t-t_0)/T] + c$, where $(t-t_0)$ is the interaction time and c is the constant background due to losses out of the CPT state $|N\rangle$. As expected, the time for trapping gets shorter for increasing intensity.

We also recorded the fluorescence intensity at certain fixed positions while scanning the frequency splitting of the laser fields. The sharp drop at two photon resonance due to CPT gets more pronounced (more atoms trapped in the $|N\rangle$ state) for longer interaction times between atoms and light. Three such scans taken at the three different positions along the atomic beam indicated in Fig. 7 are shown in Fig. 9. This set nicely shows the establishment of CPT, the corresponding CPT dip for position C reaching a contrast of up to about 90%.

Measuring the integrated fluorescence intensity, we took a series of scans of the CPT dip (Fig. 10) yielding the contrast

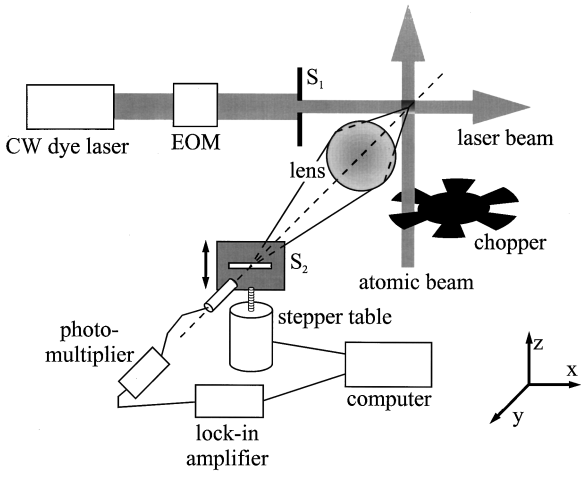

FIG. 6. Scheme of the experimental setup.

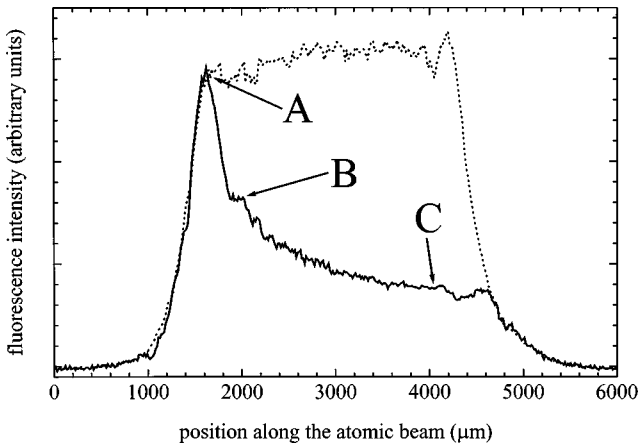

FIG. 7. Atomic beam position (time-) resolved fluorescence intensity for two different values of frequency difference for two laser light sidebands: $\delta = 1772$ MHz, solid line; $\delta = 1760$ MHz, dotted line. Position translates into time as 1 μm$\doteq$1 ns (for the mean velocity of atoms). External magnetic field unshielded ($B \approx 1$ G, $g_B = 0.07\gamma_e$), total laser intensity $I = 120$ mW/cm^2.

and linewidth of the CPT dips versus the laser intensity. We observed the decrease in contrast as well as in linewidth of the dip as the intensity decreases. At low intensities the existence of two peaks separated by about 1 MHz becomes evident. This separation is due to the magnetic field parallel to the laser polarization, which shifts the Zeeman sublevels in energy. Therefore, two separate Λ systems (with $m_F = -1$ and $m_F = +1$) with different ground level splittings are present for π excitation. From the separation one can calculate the residual parallel magnetic field to be approximately 0.8 G. The CPT dips can be observed for the laser intensities down to certain threshold, corresponding to a minimum intensity necessary for establishment of CPT [cf. Eq. (12)]. The value of this minimum intensity was 4 mW/cm^2 in our measurements, corresponding to the Rabi frequencies $g_1 = 0.14\gamma_e$ and $g_2 = 0.08\gamma_e$ ($\gamma_e = 6.3 \times 10^7$ s^{-1}) for one of the Λ systems. This means that the value of the perpendicular component of the magnetic field was less than 0.4 G, as can be estimated from Eq. (12).

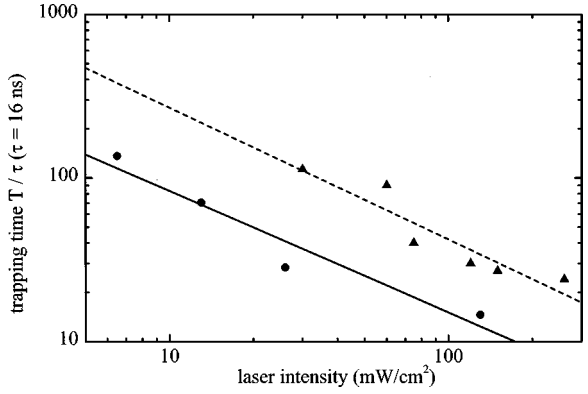

FIG. 8. Time constants for the steady-state establishment in Na at two-photon resonance versus total laser intensity. ▲, experimental points for the case without shielding of the magnetic field ($B \approx 1$ G); dashed curve, corresponding linear fit; ●, case with shielding of the magnetic field ($B \approx 14$ mG); solid curve, corresponding linear fit.

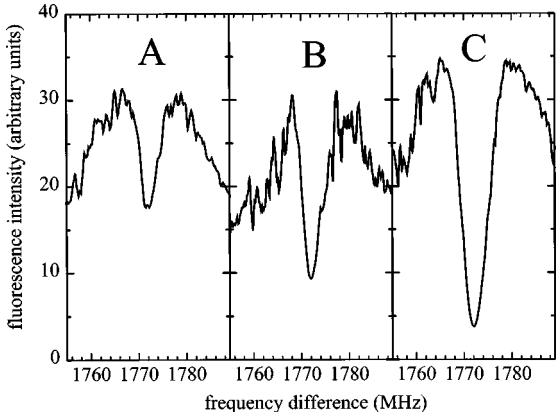

FIG. 9. Scans of the black line at atomic beam positions indicated in Fig. 7.

For a second series of measurements we enclosed the interaction region in a cylinder made of μ metal in order to shield the magnetic field. The cylinder had six holes along the three axes for the atomic beam, the laser beam, and detection, respectively. While the shielding factor perpendicular to the cylinder axis is very high, it is relatively poor along its axis. Measurements at higher fields indicated shielding factors of 200 perpendicular and 20 parallel to the axis, but in the experiment it turned out that the shielding parallel was only about 3 at the lower fields present in the actual setup. However, as the field is shielded much better perpendicularly to the cylinder axis, it means that the residual magnetic field is almost perfectly parallel to the cylinder axis and therefore also to the light polarization direction. Thus we now have ideal π excitation even with magnetic field present and almost no Larmor precession of the Zeeman sublevels popula-

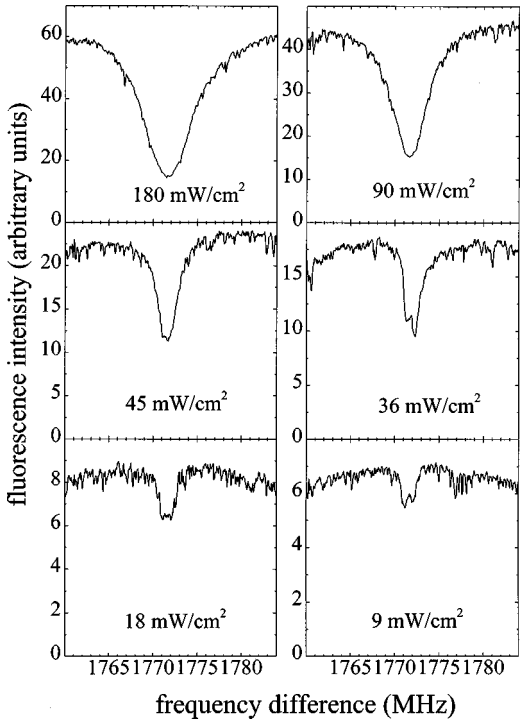

FIG. 10. Integrated fluorescence intensity spectrum for different total laser light intensities indicated in the figures for the case of unshielded stray magnetic fields.

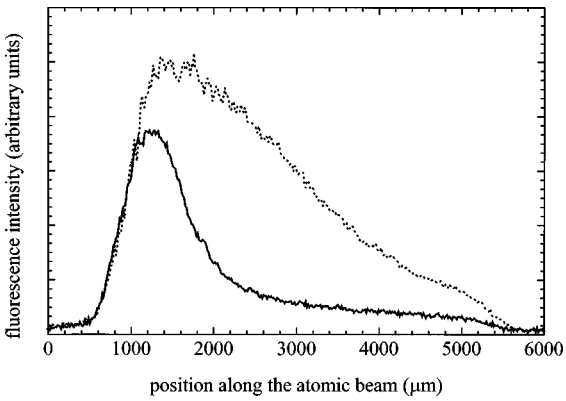

FIG. 11. Atomic beam position (time-) resolved fluorescence intensity for two different values of frequency difference for two laser light sidebands: $\delta = 1772$ MHz, solid line; $\delta = 1760$ MHz, dotted line. Position translates to time as 1 μm≐1 ns (for the mean velocity of atoms). External magnetic field shielded ($B \approx 0.014$ G, $g_B = 0.001\gamma_e$), total laser intensity $I = 26$ mW/cm^2.

tion. Provided that, now a regular dark state $F=2$, $m_F=0$ exists and atoms are pumped out of the fluorescence cycles into that state even for cases when there is no CPT at all. Therefore, the fluorescence decreases along the beam all the time, the only difference being a faster decrease for CPT present. This can be seen in Fig. 11, which is the analog to Fig. 7 (cf. solid curves in Fig. 4). As described above, we also made scans of the CPT dip for different intensities (Fig. 12). Now CPT is established for much lower intensities. The threshold minimum intensity was about 0.2 mW/cm^2, which corresponds to the Rabi frequencies $g_1 = 0.031\gamma_e$ and $g_2 = 0.018\gamma_e$ and to the perpendicular component of the magnetic field of less than 14 mG. The residual parallel magnetic field also causes the formation of two peaks, but now less separated, indicating a shielding factor of about 3. The contrast and linewidth again get smaller for smaller intensities. Compared to the case without shielding, the contrast is much higher for the shielded case, but the linewidth is more or less independent of the magnetic field (note that the linewidth always refers to one single peak of the twin peaks present in each scan). The explanation for this behavior is as follows. The linewidth is determined by the sum of the loss rate Γ_C of the coupled state $|C\rangle$ with $\Gamma_C \approx g_0^2/\gamma_e$ and the loss rate Γ_N from $|N\rangle$ (determined by the value of the magnetic field in our case) (see, e.g., Ref. [2]). However, under the condition [Eq. (12)] $\Gamma_C \gg \Gamma_N$, the linewidth is proportional to the intensity and it does not depend on the magnetic field. At the same time, the contrast is inversely proportional to the degree of imperfection of CPT [15,16], which is the ratio of Γ_N to Γ_C. Therefore, at a fixed magnetic field the contrast decreases with decreasing intensity (due to a decrease of Γ_C) and at fixed intensity it is larger for smaller magnetic fields (due to a decrease of Γ_N).

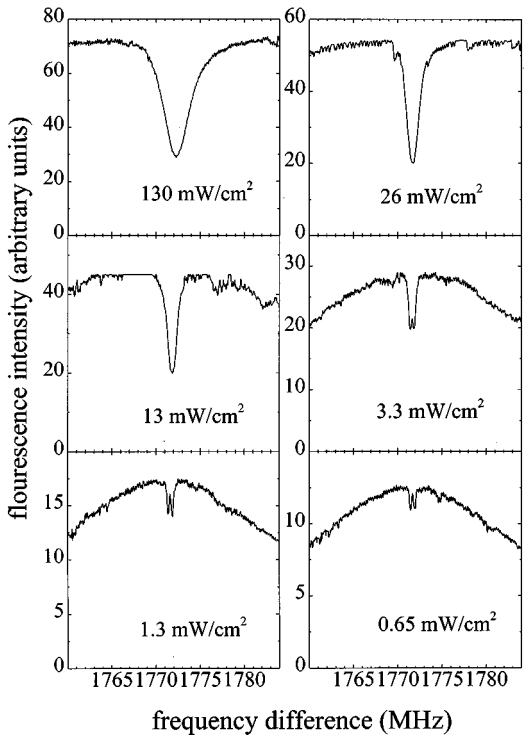

FIG. 12. Integrated fluorescence intensity spectrum for different total laser light intensities indicated in the figures for the case of shielded stray magnetic fields.

We note finally that there is no complete correspondence of the experimental results with our four-level theory developed above. For example, the transient structures of the excited-state population (Fig. 4) are not resolved in the experiment due to both finite resolution of the optics and the Maxwellian distribution of the atomic velocities. The calculated trapping times are smaller and the contrast is higher than those obtained experimentally. This especially concerns the case with a stray magnetic field present. The reason is that the magnetic field has a stronger influence on the behavior of Na atoms in the bichromatic laser light than it was assumed in the four-level model. It turns out that even moderate magnetic fields of 1 G entangle Zeeman sublevels so that all of them are involved in the process. Therefore, the four-level model fails to describe in details the dynamics of COP in such complicated real systems as Na atoms. We have performed time-dependent numerical calculations for the atomic system involving all levels of the Na D_1 line relevant for the present experiment. The calculations are based on the formalism developed in Refs. [1, 19]. The results show a coincidence with experimentally measured trapping times, the black linewidth, and the contrast within 10–15 %. However, the physical picture and the main characteristics of COP drawn by the four-level model remain valid.

IV. CONCLUSION

We have investigated both experimentally and theoretically the temporal evolution of the CPT process in a sodium atomic beam. For that purpose we first analyzed theoretically two simplified cases: the well-known closed (loss-free) three-level Λ system and a four-level system consisting of a Λ system with an additional ground state not contributing to the coherent superposition state. Here the influence of a weak magnetic field can be modeled by population precession between the states that contribute to the dark superposition state and this external state. The coupling between the CPT state and the external state induced by a magnetic field critically influences the temporal behavior of the trapping process because coupling means losses out of the trapping state.

This magnetic-field coupling also sets a lower limit for the light intensity necessary to establish CPT. Experimentally, we recorded the spatially resolved fluorescence intensity along the atomic beam (which corresponds to a temporal evolution) for cases with stray magnetic fields present and with shielding of the field, obtaining results that are in good qualitative agreement with simple theoretical model. We also recorded the fluorescence intensity at certain fixed spatial (time) positions while scanning the frequency splitting of the laser fields. The sharp drop at two-photon resonance due to CPT gets more pronounced (more atoms trapped in the noncoupled state) for longer interaction times between atoms and light. Performing measurements with different laser intensities allowed us to determine how this affects the time constant for the trapping process. The time for trapping gets shorter for increasing optical pumping rate. The CPT resonances are observed for the laser intensities down to a certain threshold, its value depending on the presence or absence of magnetic field. This corresponds to the behavior of the minimum intensity necessary for CPT establishment, which is predicted by our theory. Our analysis outlined the limits of application of the simple loss-free CPT pictures frequently used. It also showed how to model a more realistic scheme of the process while still retaining most of the physical clarity of the simple theory. Despite its simplicity, our scheme reproduces quite well the features of CPT in rather complicated realistic schemes, namely, the Zeeman level structure of sodium.

ACKNOWLEDGMENT

This work was supported by the Austrian Science Foundation under Project No. S 6508.

[1] D. E. Nikonov, U. W. Rathe, M. O. Scully, S.-Y. Zhu, E. S. Fry, X. Li, G. G. Padmabandu, and M. Fleischhauer, Quantum Opt. **6**, 245 (1994).

[2] For a review of coherent population trapping phenomenon see, B. D. Agap'ev, M. B. Gornyi, B. G. Matisov, and Yu. V. Rozhdestvensky, Usp. Fiz. Nauk **163**, 1 (1993) [Phys. Usp. **36**, 763 (1993);]; E. Arimondo, in *Progress in Optics*, edited by E. Wolf (Elsevier, Amsterdam, 1996), Vol. 35, p. 257.

[3] G. G. Padmanbandu, G. R. Welch, I. N. Shubin, E. S. Fry, D. E. Nikonov, M. D. Lukin, and M. O. Scully, Phys. Rev. Lett. **76**, 2053 (1996).

[4] P. R. Hemmer, K. Z. Cheng, J. Kierstead, M. S. Shahriar, and M. K. Kim, Opt. Lett. **19**, 296 (1994).

[5] W. Maichen, R. Gaggl, E. Korsunsky, and L. Windholz, Europhys. Lett. **31**, 189 (1995); W. Maichen, F. Renzoni, I. Mazets, E. Korsunsky, and L. Windholz, Phys. Rev. A **53**, 3444 (1996).

[6] E. A. Korsunsky, B. G. Matisov, and Yu. V. Rozhdestvensky, Zh. Eksp. Teor. Fiz. **100**, 1438 (1991) [Sov. Phys. JETP **73**, 797 (1991)].

[7] E. A. Korsunsky, B. G. Matisov, and Yu. V. Rozhdestvensky, Zh. Eksp. Teor. Fiz. **102**, 1096 (1992) [Sov. Phys. JETP **75**, 595 (1992).]

[8] M. O. Scully, Quantum Opt. **6**, 203 (1994).

[9] Y.-Q. Li and M. Xiao, Opt. Lett. **20**, 1489 (1995).

[10] M. Löffler, M. D. Pilloff, and M. O. Scully, Quantum Semiclassic. Opt. **8**, 861 (1996).

[11] A. D. Wilson-Gordon, R. Klimovsky-Barid, and H. Friedmann, Phys. Rev. A **25**, 1580 (1982).

[12] P. Tremblay and C. Jacques, Phys. Rev. A **41**, 4989 (1990).

[13] Y. Nafcha, D. Albeck, and M. Rosenbluh, Phys. Rev. Lett. **67**, 2279 (1991).

[14] Y. Nafcha, M. Rosenbluh, P. Tremblay, and C. Jacques, Phys. Rev. A **52**, 3216 (1995).

[15] M. B. Gornyi, B. G. Matisov, and Yu. V. Rozhdestvensky, Zh. Eksp. Teor. Fiz. **95**, 1263 (1989) [Sov. Phys. JETP **68**, 728 (1989)].

[16] E. Korsunsky, D. Kosachiov, B. Matisov, Yu. Rozhdestvensky, L. Windholz, and C. Neureiter, Phys. Rev. A **48**, 1419 (1993).

[17] F. Renzoni, W. Maichen, L. Windholz, and E. Arimondo, Phys. Rev. A **55**, 3710 (1997).

[18] I. I. Sobelman, *Atomic Spectra and Radiative Transitions* (Springer-Verlag, Berlin, 1979), p. 198.

[19] H. Y. Ling, Y.-Q. Li, and M. Xiao, Phys. Rev. A **53**, 1014 (1996).